Journal of Advanced Engineering Trends
ISSN : 2682 - 2091

Vol.42, No.2. July2023

http://jaet.journals.ekb.eg

TACTILE OBJECT RECOGNITION ROBOTIC SYSTEM USING SUPERVISED MACHINE LEARNING

Marwa M. Kamel[1], Abou-Hashema M. El-Sayed[2], Mohamed I. Awad[3], Gamal E.A. Abou-Elmagd[4]

[1]Mechatronics and Industrial Robotics Program, Faculty of Engineering, Minia University, El-Minia, Egypt.

E-mail: *marwakamel93@gmail.com*

[2]Electrical Engineering Department, Faculty of Engineering, Minia University, El-Minia, Egypt.

E-mail: abouhashema@mu.edu.eg

[3]Mechatronics Engineering Department, Faculty of Engineering, Ain Shams University, Cairo, Egypt.

E-mail: mohammed.awad@eng.asu.edu.eg

[4]Production and design Engineering Department, Faculty of Engineering, Minia University, El-Minia, Egypt.

E-mail: g_magd@mu.edu.eg

Abstract

This paper aims to perform shape estimation actions on 2D uniform objects such as Square, Circle, Triangle and Pentagon to predict the actual shape of the tested objects. A tactile fingertip has been used to construct the shape that encloses some pressure sensor elements (called Taxels). One advantage of this study is the taxel`s number used, which is fewer than any other types of tactile sensor in the previous related studies as well as the new proposed exploratory technique. Moreover, the collected datasets have been used as an input for the three different learning classification algorithms. k-Nearest Neighbors Classifier (KNN), Naïve Bayes and Support Vector Machine (SVM) have been implemented as supervised learning algorithms to recognize the desired object shape from the collected data. As a result, the best performance obtained with SVM is by using the Radial Basis Function (RBF) that gives an average of 96.3% accuracy in shape recognition. Not only that, another performance comparison is made by smalling the scanned area of the same tested objects; the square and circle shapes are explored in the new area because of its lower recognizing performance (94.85 % and 94.71% respectively). Thus, enhancing the accuracy to be 96.03% and 98.8% respectively which is a remarkable performance.

Keywords— *Tactile sensor; Object recognition; Classification algorithms; shape; classifier.*

1. Introduction

Touching helps us to feel and interact safely with our surroundings. Human interaction is more functional than robots by considering the surrounding environment while executing tasks. However, due to the huge need for robot interaction in human life, advances in technology have shown great progress in combining touch sensors with robot hands which mimic receptors and simulate the human hand with fingers in many applications to perform its function [1].

A few years ago, studies related to that subject were relayed mainly on a vision to detect and recognize the desired shape, Authors in [2] used a camera to enhance the prediction of surface orientation. Moreover, Kumar Rahul [3] used a vision sensor as a camera to extract an image to give the robot the ability to control and react with the pick and place operations.

Many attributes of the object such as hardness, thickness, softness, etc cannot be recognized precisely by using the vision information. Moreover, the discovered areas, such as underwater or in volcanoes, are not convenient with many restrictions to use cameras, which motivates the researchers to focus on the use of the tactile sensor instead of vision to ensure accuracy and well-performance of robot tasks by providing different circumstances of exploration [4].

Tactile sensor exploration over years has proven its effectiveness in extracting the properties of an unknown object using the concept of human touch [5] which is involved in many delicate applications. For example, huge advances in robotic surgery have been counted, referring to that a conducted survey illustrates the use of the tactile sensor in producing a multifunction electronic skin (e-skin) which depends mainly on the haptic response from those sensors [6].

A low-cost tactile sensor is used to gather the desired data which is a remarkable advantage of our study; it successfully achieves the required tasks and

Revised:13 October, 2021, Accepted:23January , 2022

proves its efficiency in collecting data as high-priced sensors such as iCub tactile sensor that performs the same tactile actions with nearly similar accuracy [7, 8].

For understanding the information experienced by touch sensors, Artificial Intelligence (AI) algorithms have been applied which have shown to be effective in a variety of applications, including object shape recognition. For categorizing contacts, many machine learning classifiers have been constructed to analyze the collected data [7], the most often used ones are naive Bayes [9], Support Vector Machines (SVM) [10], and k-Nearest Neighbour (kNN) [9].

In this paper, a new simpler technique of exploration is proposed to enhance the robot interaction and allow it to autonomously perform tasks in an unstructured environment. We succeeded in validating the easiness of the tested technique in exploring surface features (e.g. shape dimension, edges, and curvatures) keeping in mind the accuracy of classifying the shape of the object to be nearly similar to the accurate one.

Therefore, Three previously mentioned classification algorithms have been implemented to train the arm robot to predict the class of the shape (i.e. output class ϵ {0, 1}) according to the sensor readings attached to its fingertip, namely k-Nearest Neighbor (kNN), Naïve Bayes classifier, and Support Vector Machine (SVM). The accuracy is calculated by dividing the true predicted classes by all of the sample's class numbers. The approach`s performance is validated on several explored shapes, indicating that it works robustly and directly on all tested objects, It also has the potential to identify more complicated shapes with more sophisticated control.

2. Experimental setup

2.1. Robotic Platform

ST Robotics R-12 arm robot is used to perform precise positioning movements in proposed recognition tasks, The R-12 model has a length of 500 mm, five degrees of freedom similar to a human arm with a 360-degree rotating base, and the workspace is 1000 mm spherical diameter [16]. For more details see the manual [17]

The robot platform is constructed to enable shape extraction in specified coordinates; X Y Z axes. The body of the arm is fixed on a pre-settled dimensional table concerning arm workspace as shown in fig.1. The explored area's dimensions are set to 100x100 mm, which is the arm's reachable range's maximum linear distance (spherical workspace); it is picked after some experimental attempts. Hence, accurate linear movements in exploration tasks are guaranteed.

Recently, by applying different technologies in the exploration process, the research has made a great contribution to shape recognition using tactile sensors. Pezzementi et al [11] presented a sequential state estimation technique that successfully classified the object's global identity by applying sequential pressing at random points on the desired object using a tactile array sensor. Contour following technique is also one of the most tested techniques that proved its efficiency in exploring different shapes by tracking the edges actively to estimate the dimension and orientation of the object [12-15].

The entire system components and their connections are labelled in Fig.2. It illustrates the connections between the R12 robotic arm and the tactile sensor; the robot movements are controlled by the tactile feedback signal provided by the sensor. The gathered dataset of the target shape has been analyzed by using Matlab software on PC. For further clarification, the arm robot movements depend mainly on the tactile sensor signals analyzed by the Arduino. When the sensor detects contacting pressure, it sends the signal to the Arduino using the I2C protocol. After processing the reading data, commands are sent to the controller of the arm robot to move by energizing the stepper motors with its drivers to reach the next desired step (step length is y=5mm, x=3mm); these commands are established by the interface window of Matlab Software.

Fig. 1: ST arm robot with Takktile fingertip attached in end-effector.

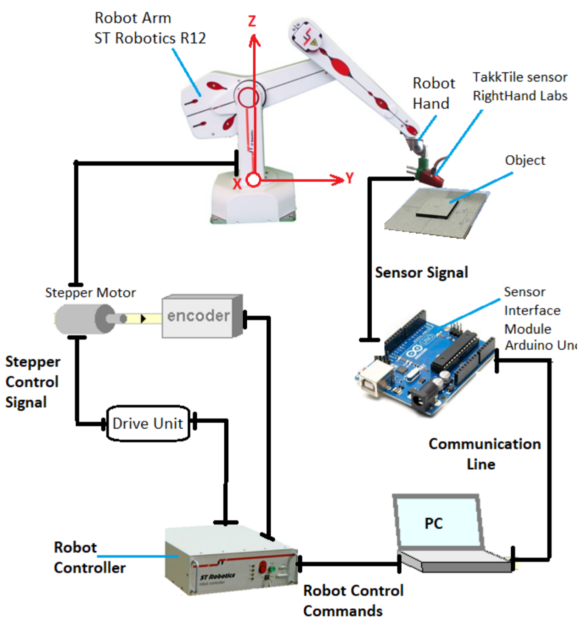

Fig. 2: Block diagram of the robotic tactile sensor system

2.2. Tactile fingertip sensor

The tactile version used here is called TakkTile fingertip developed by Right-Hand Labs [18], it was integrated both electrically and mechanically into the fingertip of the previously mentioned arm robot as an end effector.

TakkTile is a cost-effective barometric sensor embedded in rubber that is used to sense contact forces. It has 6 contact pads arranged in a 2x3 array called taxels as shown in fig.3. Each taxel is made of a 5x3mm pressure sensor of type MPL115A2, as shown in fig.4, with a maximum sensing range up to 177 kPa [19]. When a force is applied to the sensor during surface contact, it increases the parametric pressure reading. Hence, the taxel deflections can precisely characterize the contact location, edges, and curvatures. Then, the data is transmitted over an I2C bus communication to Arduino. This clearly illustrates the sensor principle of operation. The fingered robotic hand was simulated to be similar to a human hand. As a result, employing the sense of touch gives the robot feelings about its surroundings. [20].

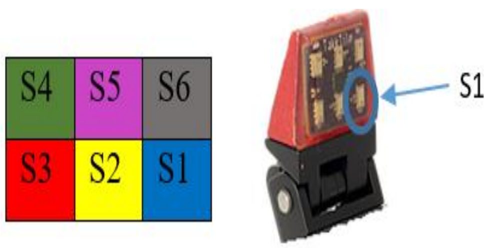

Fig. 3: Taxel geometry of TakkTile sensor

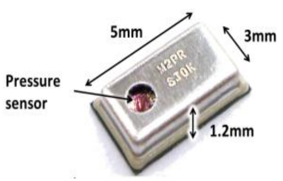

Fig. 4: Taxel dimensions

2.3. Finger positioning for data collection

In this work, a new tactile exploration technique is executed and validated its efficiency in predicting the actual 2D shape of the object. Scanning the whole explored area technique, in a pattern shown in fig.5 (A), is one of the simplest procedures that ensure high precision, unlike the other used techniques that require complex software to ensure low vibration and accurate recognition. Consequently, it gives a brief view of the surface curvature of the object that is going to help in future 3D exploration works.

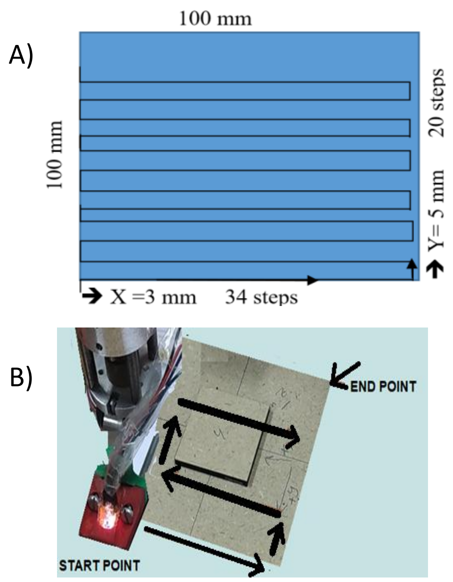

Fig. 5: The proposed exploratory technique to collect data. A) Scanned area Dimension and step length X=3mm, Y=5mm. B) Fingertip movements to explore the tested object (square)

Based on fingertip taps, tactile datasets are systematically collected. It compose pressure readings of the 6 taxels and their corresponding position in the XY axis as well as the output class. A flow chart demonstrates the entire procedure of the steps followed to predict the actual shape is shown in fig.6. The following steps illustrate the section related to the way of data collection used for recognizing approaches:

1- Regarding the selected fixed boundaries of the scanned area (100x100 mm), the starting and ending point positions are fed to the arm as shown in fig.5 (B)
2- The axes direction of moving is settled with respect to the arm coordinates and its axes as shown in fig.7

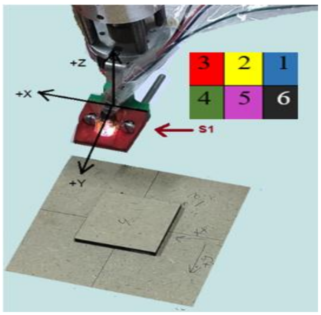

Fig .6: Specified Taxel`s colours of Takktile fingertip and its coordinates relative to arm platform

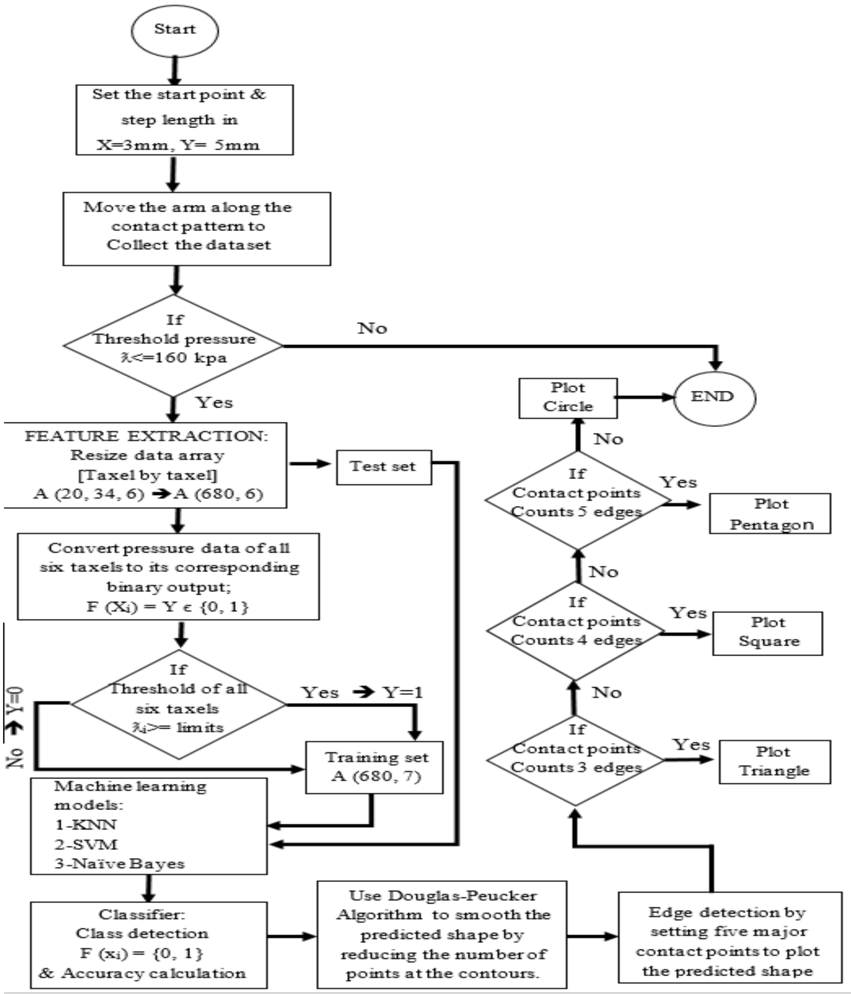

Fig. 7: Perception action procedures for the proposed new technique

3- According to the taxel dimension (5x3 mm) [19] and to ensure high tactile image resolution by minimizing the step as possible as we can, the single step of the finger tap is chosen to be in X=3mm and in Y=5mm.

4- While tapping, a threshold pressure value (ƛ ≤ 160 kpa which is below the max sensing value of the used sensor) is chosen to respond actively with tactile contacts and take the decision whether to continue pressing or stop tapping whenever pressure exceed the limits and save the reading pressure value of taxels. This is done to avoid collisions or any potential damages to the fingertip or the arm

5- A sequence of steps is done horizontally and vertically until reaching the endpoint as shown in fig.5 (B). An array of 20x34x6 has been extracted and sampled as the pixelated image (i.e. 20x34 pixels per each taxel) where the resolution of the pixel is 5x3 mm.

6- The dataset is arranged in a readable form by the classifier where each input data of one pixel should be presented in a row and all the sensor`s data of the same taxel listed in a column. Thus the 20x34x6 array is converted to an array of 680x6 (680 pixels containing pressure readings of 6 taxels (pins in the TakkTile sensor)), this is done for all collected datasets of all tested objects.

7- The training dataset (680x7) is prepared by converting the pressure data of all six taxels to its corresponding binary output; F (X_i) = y ϵ {0, 1} depending on the value of threshold of each taxel. Then fed it to the classifier for training execution. Table 1 below illustrates a part of the collected data of pixels in the tactile image of the circle shape (6 taxels per pixel) and its output class; whether it is 0 or 1 according to the threshold value of each taxel.

Table 1: Converting pressure readings of some pixels to binary output class of circle

Pixel no	Taxel 1 (S1)	Taxel 2 (S2)	Taxel 3 (S3)	Taxel 4 (S4)	Taxel 5 (S5)	Taxel 6 (S6)	Output class (y)	X (mm)	Y (mm)	Threshold (ƛ)
558	97	39	63	104	65	73	0	39	80	If (ƛ1 > 98 & ƛ2 > 40 & ƛ3 > 64 & ƛ4 > 105 & ƛ5 > 66 & ƛ6 > 74) Print y=1 Otherwise, Print y=0
559	97	39	63	104	65	73	0	42	80	
560	**100**	**44**	**68**	**110**	**68**	**76**	**1**	45	80	
561	100	44	68	107	68	76	1	48	80	
562	100	44	68	106	68	76	1	51	80	
563	100	44	68	110	69	76	1	54	80	
564	97	39	63	105	65	73	0	57	80	

2.4. Classification

In this paper, a comparison between three different classification algorithms for exploration tasks has been done to observe the best one in terms of accuracy and shape prediction as near to the true one as feasible. To do that, a set of 680 samples of input data per each taxel in the tactile sensor, i.e. 6 contact pads (taxels), are arranged in a 680x6 array where each row represents a point called pixel as an image, each pixel has its coordinates in XY axis. Another column is added to the array that represents the class label whether it is 0 or 1; where 0 stands for no object at that point and 1 stand for sensing an object at this point (see the previous section) considering the threshold value.

The processed data A(680x7) for each object is used to train the classifier by applying ML algorithms toolbox in Matlab software; feeding the 680x6 array as predictors and the rest column 680x1as an output class of each pixel. After that, the testing phase was executed by feeding a newly collected data of the same or different shape (e.g. same shape dimension collected in different environmental circumstances such as sensor deformation or pressure contact) to predict the output class label with its known orientation and hence ensure the exploration`s success. See fig.6.

2.4.1. K-Nearest Neighbor classifier (KNN)

KNN is the most popular classification algorithm used in large datasets. Making a simple majority vote of the k nearest neighbors of each tested point is the way to perform the classification. To illustrate, the distance between an undefined point and the clusters of the pre-classified data is measured to report the label of that point relaying on its proximity to one of the clusters, thus to compute the distance Euclidean formula was used [9,21].

$$Distance\ Function = \sqrt{\sum_{i=1}^{k}(X_i - Y_i)^2} \quad [22]$$

Where {X, Y} is a pair of pixel orientation in XY axis that belongs to the K neighbors points used to predict the new class label yϵ{0 1}. In this work, the value of the nearest neighbors is chosen to be k=5 that produces the best performance, see table 2.

2.4.2. Naïve Bayes

Naive Bayes classifier is one of the most sophisticated methods used in machine learning techniques. It uses a statistical inference based on the theorem of probability (Bayes theorem) with strong independent assumptions to get the best output classes [9].

Using the formula of Bayes Theorem as stated below, the datasets are trained to predict the correct class and then tested on the new dataset to estimate the desired shape [21].

$$p(Y = C_k | X = x) = \frac{P(X=x|Y=C_k)P(Y=C_k)}{P(X=x)} \quad [22]$$

Where, Y is a discrete variable that falls into exactly one of the output possible classes $\{C_k\} = \{0\ 1\}$ for $k \in \{1,\ldots K\}$; here K=2. The features of X1,..., Xd can be any discrete or continuous attributes; $X=[\ X_1\ X_2\ X_3\ X_4\ X_5\ X_6]$ input pressure readings of 6 taxels. P (Y|X) is a posterior probability for possible values of class Y and P(X|Y), the probability density (likelihood) of predictors X given class label Y.

Two different functions of naïve Bayes, (Normal (Gaussian) distribution and Kernel density estimation function) have been implemented to ensure the best shape fitting, see table 2.

2.4.3. Support Vector Machine (SVM)

Another commonly used classification algorithm is SVM, which mainly works on non-linear datasets by generating a hyper-plan called decision boundary that separates between different classes. By using kernel function, the dimensional input space can be converted from low to high and hence produce a separable dataset that can be simply classified into its corresponding classes. Those Kernel functions are called linear function, RBF (Radial Basis Function), etc. The best hyper-plan is chosen depending on the max-margin which is the distance between the nearest point and the examined hyper-plan [21]. The following equation is used to classify input data (x)

$$C = \sum \alpha_i y\,(s_i, x) + b \quad [23]$$

$$y(x_i) = \begin{cases} 1, & if\ s.x + b \geq 0 \\ 0, & if\ s.x + b < 0 \end{cases} \quad [23]$$

Where s_i is the hyper-plane vector, y denotes the class label corresponding to each input vector (x), weights αi, and bias b are the calculated coefficients. The linear kernel is used in this study; if $c \geq 0$, then x is classified as a member of the first group, otherwise it is classified as a member of the second group.

3. Result and Discussion

Four different soft wooden objects with chosen random dimensions (square 4 cm, circle 6 cm diameter, right-angled triangle 5 cm each side and pentagon with 2cm side length) were used to collect distinct sets of training and testing data. The tested objects were chosen to be highly salient to be easily explored, where, the material of the object does not pose any difficulties in the exploration tasks because the sensor is covered with sticky rubber. This experiment was repeated many times for each object to ensure the validity of those datasets and to reduce the noise by using the tapping technique to form a dataset consisting of 680 samples per taxel.

Using Matlab software and its Machine Learning Toolbox, two distinct datasets are collected for each object except the square has four different datasets, one of the datasets was used for training the classifier and the other for testing. Fig.8 below illustrates part of those data collected over the edges, surface and air regions (all pressure values measured at y=50mm of the circle and square shape and at y=60 mm of triangle and pentagon) the pressure values differ from one region to another as shown, so it is a good idea to enrich our study with a good data about the curvature and the boundaries of the tested objects.

After the training was executed, each classifier is tested using a different dataset of the same tested object or another object and the one that has the higher performance is tested again by feeding the dataset of each explored object, hence ensuring the highest accuracy to estimate the actual shape of that object

The predicted output classes label of each pixel is compared with the actual ones by calculating the accuracy using the below equation

$$accuracy\ \% = \frac{TP + TN}{TP + TN + FP + FN} * 100$$

Where TP and TN refer to the True Positive and True Negative classes (sum of all true classes) and FP, FN stands for False Positive and False Negative (the false predicted classes), the calculated accuracy values have listed below in Table 2. As illustrated, two different functions in Naïve Bayes (Normal (Gaussian) distribution, Kernel density estimation) and SVM algorithms (Linear Function, Radial Basis Function (RBF)) were tested to ensure a precise decision making of the best Classification Algorithm.

Table 2: Comparative performance of some classification algorithms using different parameters in predicting the shape of Square, Circle, Triangle, and Pentagon objects

Classification Algorithms	Square	Circle	Triangle	Pentagon	Mean accuracy	Time (sec)
KNN (K=5)	83.24%	85.88%	93.53%	93.68%	90.33%	1.01s
Naïve Bayes (Normal (Gaussian) distribution)	86.03%	76.03%	98.38%	97.79%	89.56%	0.41s
Naïve Bayes (Kernel density estimation)	83.97%	84.12%	55.4%	98.97%	80.62%	2.60s
SVM (Linear Function)	90.59%	85.4%	99.02%	99.1%	93.53%	2.81s
SVM (RBF)	94.85%	94.71%	99.41%	99.4%	97.09%	9.55s

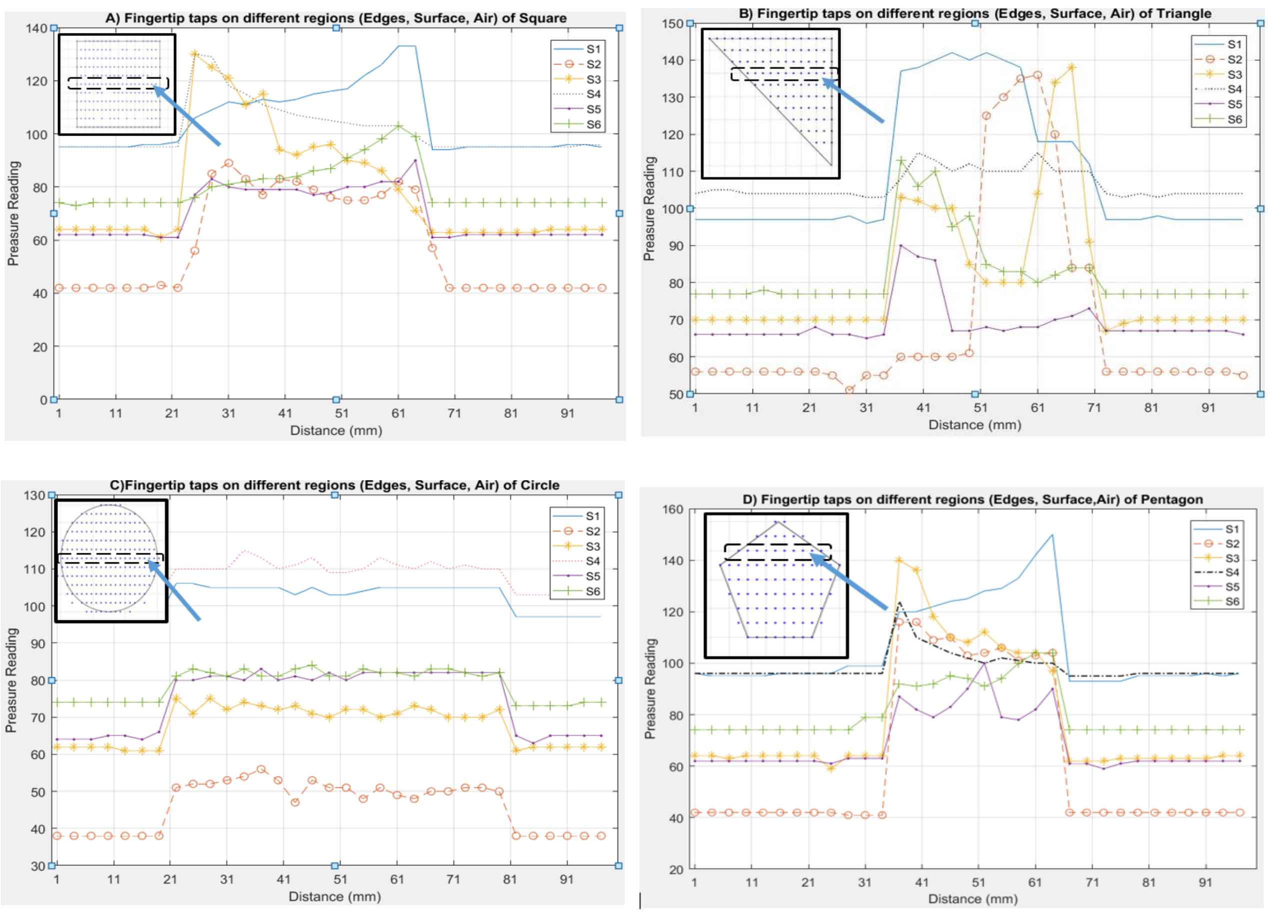

Fig. 8: The pressure variance of 6 taxels tapping over different tested objects in different regions; (A) square at Y= 50mm, (B) triangle at Y= 60mm (C), Circle at Y = 50mm and (D) Pentagon at Y= 60mm. The figure presented at the upper left side of the graph refers to the plotted section (all the data collected at a point in Y-axis)

From that comparison, we concluded the best performance of the tested algorithms in predicting the true shape of the four desired objects which is the Support Vector Machine (SVM) algorithm using RBF function with a mean accuracy of 97.09%. However, the average computation time of that classifier is about 3 times more than the time required for the other classifiers.

As listed in the flow chart shown in figure 6, the next step is executed to plot the estimated shape to get it nearly similar to the actual one. This is approached by using the Douglas-Peucker (DP) Algorithm which is one of the most popular methods used for simplifying the curve by choosing the most significant points of a curve and neglecting the others (less important points) to smooth the estimated shape [24, 25]. The degree of simplification depends on selecting an effective value of simplification tolerance ϵ (epsilon); we tested different values (3, 5, 10, 20, and 30) to get the best shape estimation at Ɛ=20.

$$\varepsilon = \frac{T}{100} \times \sum_{i=1}^{N-1} D(P_{i+1}, P_i) \qquad [26]$$

Where, $D(P_{i+1}, P_i)$ is Euclidean distance between two points p_{i+1} and p_i chosen at the outer frame of the tested shape; (i.e. all the selected points to form the data series of DP is chosen to form the outer frame of the target shape neglecting the inner points collected from scanning the desired area. This is done by calculating the distance from the centre point of the shape), N is the number of points in the data series and T is a real number that varies the value of epsilon. The best estimation was done by ϵ=20, fig.9 (B) below shows the predicted shape when applying the DP algorithm where the blue circles represent the significant points to detect the shape.

Further simplification, the method applied to the estimated shape as shown in fig.9 (C), is specifying 5 major contact points that are used to determine the edges of the shape (outer frame). By counting those edges, the shape can be easily estimated (see fig.6). The way used for edge decision is by comparing the pressure reading values of the taxels at that specified point (pixel) with its near points, hence deciding whether it’s a sharp edge, as in a square, or fine edge, as in a circle.

Using the pre-known pixel`s coordinates, the predicted shape of the explored objects obtained from the SVM (RBF) algorithm was plotted in the XY-plane curve using Matlab graphs, as shown below in fig.(10, 11,12,13). It is compared with the actual (true) shape. In addition, the output classes of each object are classified in a confusion matrix below to understand the mean of overfitting, under-fitting and well-fitting curve, in other words, the matrix presents the counts of each class in the true positive and true negative.

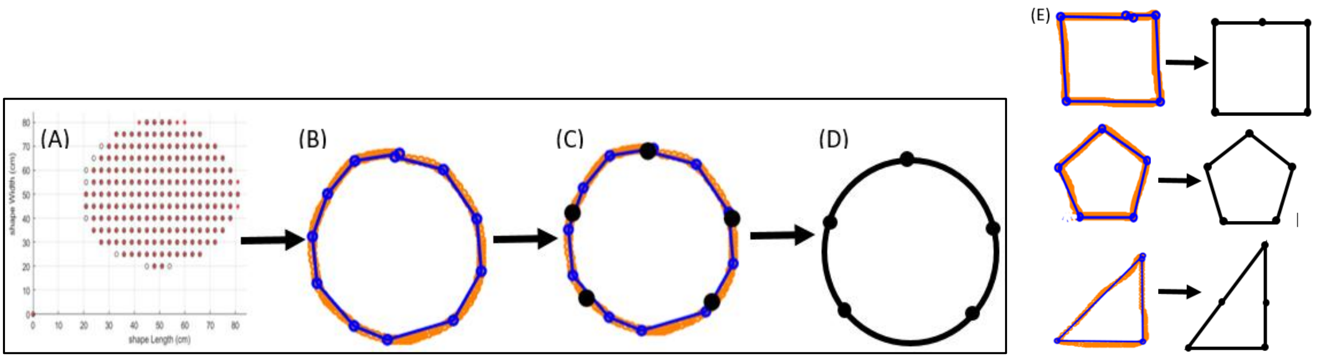

Fig. 9: Shape estimation process after successful classifying. A) Data collected from scanning surface, B) Applying DP algorithm Ɛ=20 (blue dots), C) Selecting 5 significant points to detect the edges (black dots), D) Estimating the true shape (sharp edges=0 ➔it’s a circle E) The rest of estimated shapes

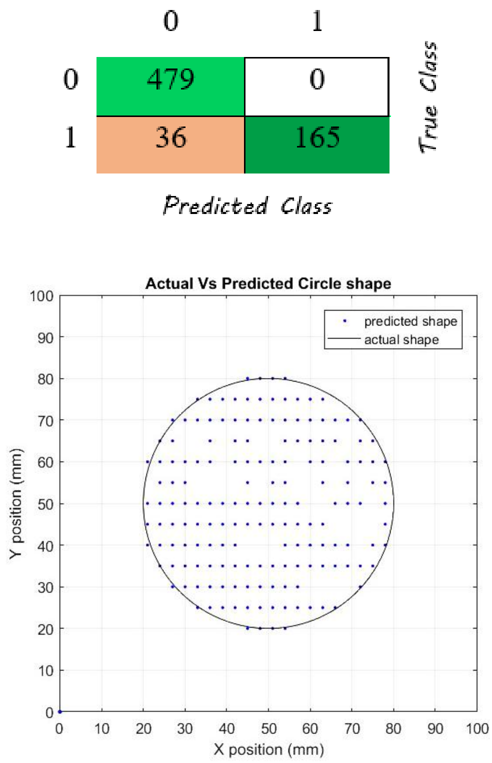

Fig. 10: Performance with confusion matrix of SVM (RBF kernel Function) classifier to predict the true Circle shape. Accuracy (94.71%)

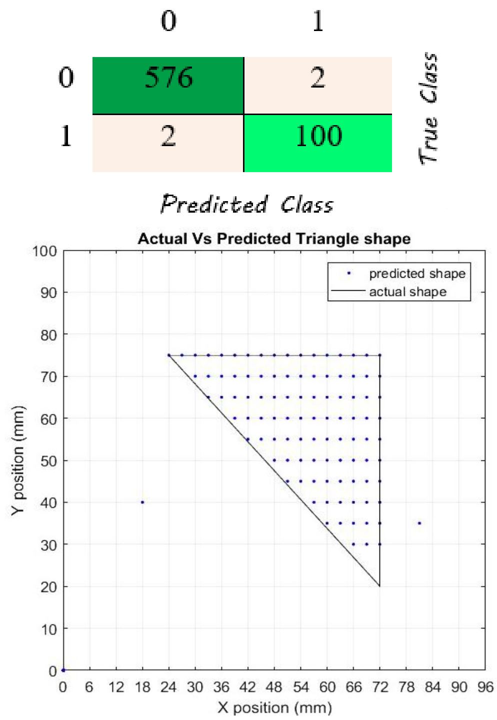

Fig. 12: Performance with confusion matrix of SVM (RBF kernel Function) classifier to predict the true Triangle shape. Accuracy (99.41%)

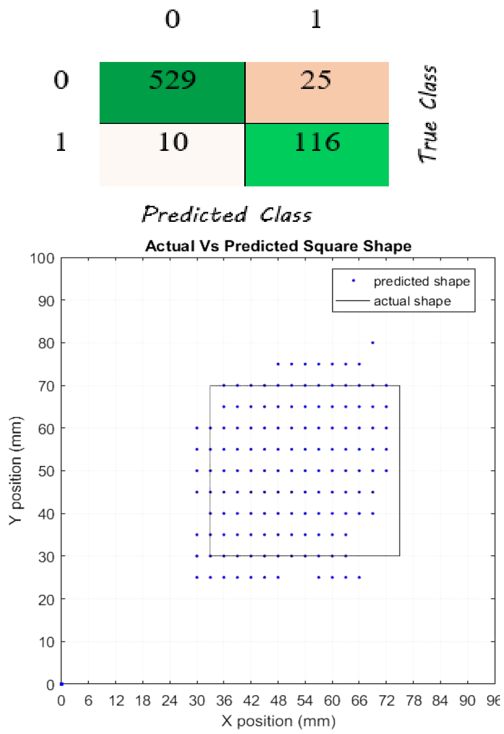

Fig. 11: Performance with confusion matrix of SVM (RBF kernel Function) classifier to predict the true Square shape. Accuracy (94.85%)

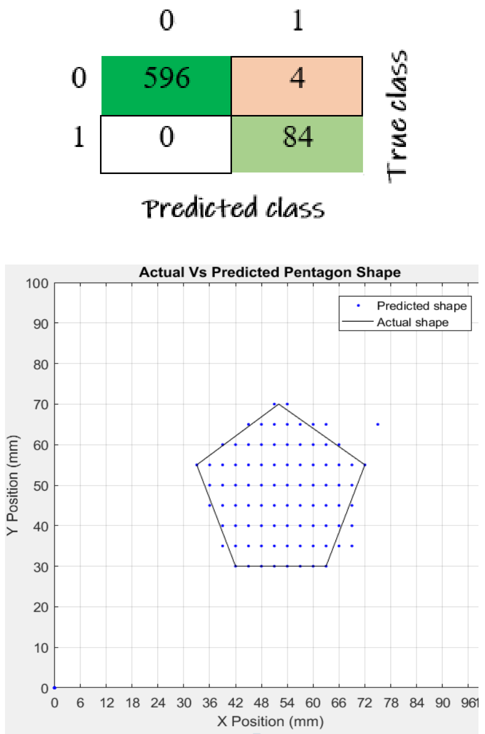

Fig. 13: Performance with confusion matrix of SVM (RBF kernel Function) classifier to predict the true Pentagon shape. Accuracy (99.40%)

To enhance the results another experiment was executed by reducing the scanned area to be 70x80 mm to decrease the dimensions of each pixel to be 2x2 mm (instead of 5x3 mm) and hence come up with better performance when exploring the desired objects. Square and circle objects were tested in this experiment since it have the lowest value of accuracy when SVM (RBF) algorithm is used. The same data array as mentioned previously of 20x34x6 elements is conducted and then arranged in an acceptable form by classifier (680x6 array). The same training and testing procedures were executed to come up with the output classes. The predicted classes of the square and circle shape are compared with the actual ones to get an accuracy of 96.03% and 98.8%, respectively, which is higher than the previously calculated value (94.85 % and 94.71% respectively). Therefore, we can conclude that by reducing the scanned pixel dimension, the exploration performance increases and hence predict successfully the actual shape as shown in fig.14 and fig.15.

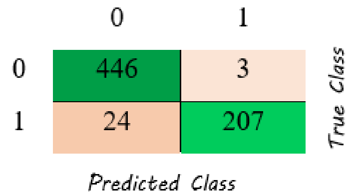

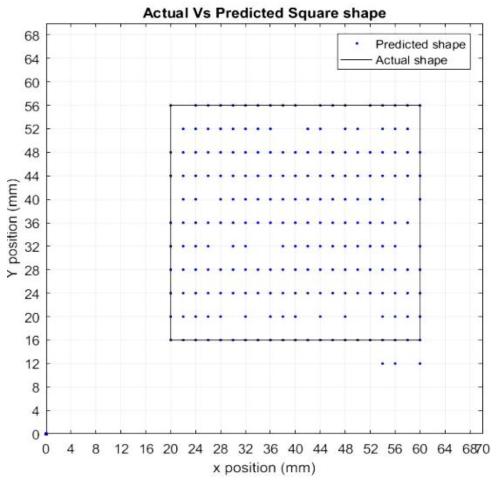

Fig. 14: Performance of SVM (RBF kernel Function) classifier to predict the true Square shape. Accuracy (96.03%)

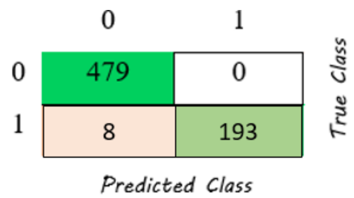

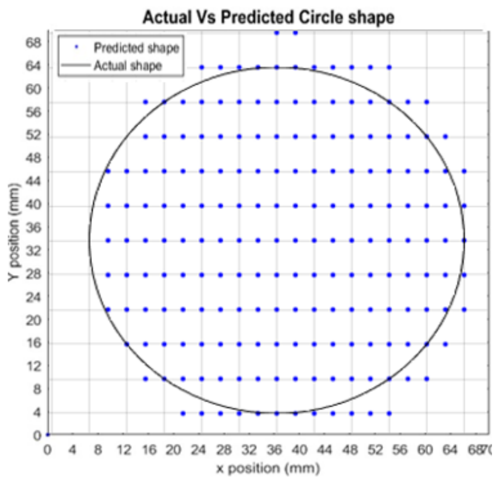

Fig. 15: Performance of SVM (RBF kernel Function) classifier to predict the true Circle shape. Accuracy (98.8%)

This proposed exploratory technique shows a significant contribution in object recognition tasks in either accuracy of perception or the efficiency of the data collection using affordable price tactile sensor regards the previously used methods. When comparing the performance of the proposed approaches, SURF-SVM and CNN-SVM, which have an accuracy of 80% and 91.67%, respectively, presented in [27] with the one presented here, the proposed scanning technique used in this work the applying conventional SVM algorithm has proven to be more accurate in predicting the tested shapes with a 97.09% accuracy.

Another remarkable notice is that in [28] the authors use high price tactile sensor (TacTip) to classify circle shapes (110mm diameter) using a histogram likelihood model to analyze a 30x30 pixel image (900 pixels) that collected by following the shape contours wherein proposed method 680 pixels only constructed per each tested shape by using lower price sensor (Takktil) and high similar accuracy have been reached in recognizing the shape. Moreover, in [29], despite using 5x9 pressure elements in a sensor to classify simple six shapes, an overall accuracy of 97.5% has been calculated which is nearly similar to our calculated one (97.09%) where our sensor has 2x3 elements (more taxels leads to accurate tactile readings per each pixel).

4. Conclusion

Four different learning algorithms were trained and tested with the Takktile sensor by tapping each pixel in the desired tested area including our object to detect a change in pressure reading depending on the explored region; edges, surface plan and air by the proposed technique. The SVM classification with the RBF function presents a good performance in estimating all the shapes with a mean classification accuracy of 97.09%. A further suggestion of a simple scanning technique in a smaller area with the same number of steps as well as using low price sensor provides a good impact in the intelligent robotic system capable of sensing different shapes in 2D or 3D as a future working.

5. References

[1] S. J. Lederman and R. L. Klatzky, "Hand movements: A window into haptic object recognition," *Cognitive Psychology*, vol. 19, no. 3, p. 42–368, 1987.

[2] H. Koch, A. König, K. Kleinmann, A. Weigl-Seitz and J. Suchý, "Predictive robotic contour following using laser-camera-triangulation," in *IEEE/ASME International Conference on Advanced Intelligent Mechatronics (AIM)*, 2011.

[3] R. Kumar, S. Lal, S. Kumar and P. Chand, "Object Detection and Recognition for a Pick and Place Robot," in *Asia-Pacific World Congress on Computer Science and Engineering*, 2014.

[4] Z. Kappassov, J.-A. Corrales and V. Perdereau, "Tactile sensing in dexterous robot hands — Review," *Robotics and Autonomous Systems*, vol. 74, no. 1, pp. 195-220, 2015.

[5] N. F. Lepora, . A. Church, C. de Kerckhove, R. Hadsell and J. Lloyd, "From Pixels to Percepts: Highly Robust Edge Perception and Contour Following Using Deep Learning and an Optical Biomimetic Tactile Sensor," *IEEE Robotics and Automation Letters*, vol. 4, no. 2, pp. 2101-2107, 2019.

[6] Y. Al-Handarish, O. M. Omisore, T. Igbe, S. Han, H. Li, W. Du, J. Zhang and L. Wang, "A Survey of Tactile-Sensing Systems and Their Applications in Biomedical Engineering," *Advances in Materials Science and Engineering*, vol. 17, 2020.

[7] W. Becari, L. Ruiz, B. Evaristo and F. J. Ramirez-Fernandez, "Comparative analysis of classification algorithms on tactile sensors," *IEEE International Symposium on Consumer Electronics (ISCE)*, pp. 1-2, 2016.

[8] A. Schmitz, M. Maggiali,, L. Natale, B. Bonino and G. Metta, "A tactile sensor for the fingertips of the humanoid robot iCub," in *IEEE/RSJ International Conference on Intelligent Robots and Systems*, 2010.

[9] S. Datta, A. Khasnobish, . A. Konar, D. N. Tibarewala and R. Janarthanan, "Object shape and size recognition from tactile images," in *2013 International Conference on Control Communication and Computing (ICCC)*, 2013, pp. 16- 21.

[10] J. M. Gandarias, A. J. García-Cerezo and J. M. Gómez-de-Gabriel, "CNN-Based Methods for Object Recognition With High-Resolution Tactile Sensors," *IEEE Sensors Journal*, vol. 19, no. 16, pp. 6872-6882, 2019.

[11] Z. Pezzementi, C. Reyda and G. D. Hager, "Object mapping, recognition, and localization from tactile geometry," in *IEEE Int. Conf. on Robotics and Automation*, 2011.

[12] U. Martinez-Hernandez, T. J. Dodd, M. H. Evans, T. J. Prescott and N. F. Lepor, "Active sensorimotor control for tactile exploration," *Robotics and Autonomous Systems*, vol. 87, pp. 15-27, 2017.

[13] L. Merker, S. J. Fischer Calderon , M. Scharff, J. H. Alencastre Miranda and C. Behn, "Effects of Multi-Point Contacts during Object Contour Scanning Using a Biologically-Inspired Tactile Sensor," *Sensors*, vol. 20, no. 7, p. 2077, 2020.

[14] N. Pestell, B. Ward-Cherrier, L. Cramphorn and N. F. Lpoa, Tactile exploration by contour following using a biomimetic fingertip, Spring International, 2016.

[15] E. A. Stone, N. F. Lepora and B. A. Barton, "Learning to Live Life on the Edge: Online Learning for Data-Efficient Tactile Contour Following," in *2020 IEEE/RSJ International Conference on Intelligent Robots and Systems (IROS)*, 2020, pp. 9854-9860.

[16] A. B. HUMBER, P. A. Deshmukh and M. S. Kadam, "The Review of Articulated R12 Robot and Its Industrial Applications," *international Journal of Research in Engineering & Technology,* vol. 2, pp. 113-118, 2014.

[17] "R12 robot arm," ST Robotics International, [Online]. Available: https://strobotics.com/small-articulated-robot.htm.

[18] "TakkTile Sensors," RightHand Robotics, Inc, [Online]. Available: https://www.labs.righthandrobotics.com/robotiq-kit. [Accessed 2020].

[19] Y. Tenzer, R. D. Howe and L. P. Jentoft, "Inexpensive and Easily Customized Tactile Array Sensors using MEMS Barometers Chips," IEEE R&A Magazine, UK, 2012.

[20] "D. Vogt, Y. Menguc, Y. Park, and M. Wehner, “Progress in Soft, Flexible, and Stretchable Sensing Systems,” Biorobotics.Harvard.Edu, pp. 0-1, 2013.".

[21] C. C. Aggarawal, DATA CLASSIFICATION: ALGORITHMS AND APPLICATIONS, CRC Press, 2014.

[22] D. S. Sayad, "An Introduction to Data Science," [Online]. Available: https://www.saedsayad.com/classification.htm.

[23] X. Yin, B. W.-H. Ng, B. M. Fischer, B. Ferguson and D. Abbott, "Support Vector Machine Applications in Terahertz Pulsed Signals Feature Sets," vol. 7, no. 12, pp. 1597-1608, 2007.

[24] L. Fernandes and B. R. Shivakumar, "Identification and Sorting of Objects based on Shape and Colour using robotic arm," in *2020 Fourth International Conference on Inventive Systems and Control (ICISC),*, 2020.

[25] A. Miller, A. Mooreand and G. Leonard, "From generalisation to segmentation: Douglas-Peucker-Ramer and movement data," *The University of Auckland*, Sep 2019.

[26] R. Zarei, . J. He, . S. Siuly , . G. Huang and Y. Zhang, "Exploring Douglas-Peucker Algorithm in the Detection of Epileptic Seizure from Multicategory EEG Signals," *BioMed research international,* vol. 2019:5173589, 2019.

[27] J. M. Gandarias, J. M. Gómez-de-Gabriel and A. García-Cerezo, "Human and object recognition with a high-resolution tactile sensor," in *2017 IEEE SENSORS*, 2017, pp. 1-3.

[28] N. Pestell, J. Lloyd, J. Rossiter and N. F. Lepora, "Dual-Modal Tactile Perception and Exploration," *IEEE Robotics and Automation Letters,* vol. 3, no. 2, pp. 1033-1040, 2018.

[29] H. liu, X. Song, T. Nanayakkara, L. D. Seneviratne and K. Althoefer, "A computationally fast algorithm for local contact shape and pose classification using a tactile array sensor," in *2012 IEEE International Conference on Robotics and Automation*, 2012, pp. 1410-1415.

ملخص البحث:

تهدف هذه الورقه البحثيه إلى التعرف على أشكال الأجسام ثنائيه البعد من خلال تنفيذ بعض العمليات الإستكشافيه للتنبؤ بالشكل الفعلي للإشكال المراد اختبارها مثل المربع والدائره والمثلث. ويتم ذلك بإستخدام حساس لمسي مكون من عدة مستشعرات للضغط ومثبت على أطراف الأصابع. إحدى ميزات هذه الدراسه هوعدد مستشعرات الضغط الموجوده في الحساس اللمسي المستخدم حيث أنه أقل من أي عدد موجود في الحساسات اللمسيه الأخرى المستخدمه في الدراسات السابقه ذات الصله. لتحليل البيانات التي تم جمعها والتعلم من خلالها تم إستخدام ثلاث خوارزميات مختلفه وهي

Nearest Neighbors Classifier (KNN), Naïve Bayes and Support Vector Machine (SVM)

وبعد اجراء بعض الإختبارات في التعرف على الأشكال تم التوصل الي ان كفاءه خوارزميه SVM هي الأعلى من بين الخوارزميات الأخرى المستخدمه وتتمثل بمتوسط دقه يصل إلى ٩٦.٣%. ولتحسين هذه الكفاءه تم إجراء تجربه أخرى تتمثل في تقليل الأبعاد التي يتم مسحها للتعرف علي الشكل المراد ولإثبات هذا علي سبيل المثال تم إستخدام المربع حيث أنه أقل دقه من بين جميعهم (٩٤.٨٥%) وتم التوصل إلى دقه أعلى ٩٦.٠٣% بعد اجراء هذه التجربه.